A Speed Sensorless Vector Control for Permanent Magnet Synchronous Motors based on an Adaptive Integral Binary Observer

Yang-Kwang Choi† , Young-Seok Kim* and Yoon-SeoK Han**

Abstract - This paper presents sensorless speed control of a cylindrical permanent magnet synchronous motor (PMSM) using the adaptive integral binary observer. In view of the composition with a main loop regulator and an auxiliary loop regulator, the normal binary observer has the feature of chattering alleviation in the constant boundary layer. However, the steady state estimation accuracy and robustness are dependent upon the thickness of the constant boundary layer. In order to improve the steady state performance of the binary observer, a new binary observer is formed by the addition of extra integral dynamics to the existing switching hyperplane equation. Also, because the parameters of the dynamic equations such as machine inertia or viscosity friction coefficient are not well known and these values can be changed during normal operations, there are many restrictions in the actual implementation. The proposed adaptive integral binary observer applies an adaptive scheme so that the observer may overcome the problems caused by using dynamic equations. The rotor speed is constructed by using the Lyapunov function. The observer structure and its design method are described. The experimental results of the proposed algorithm are presented to prove the effectiveness of the approach.

Keywords: Adaptive Integral Binary Observer, PMSM, Sensorless

1. Introduction

The permanent magnet synchronous motor (PMSM) is receiving increased attention for many industrial applications because of its high torque to inertia ratio, superior power density, and high efficiency. In order to control the PMSM, it is necessary to know the absolute position of the rotor. An absolute encoder or resolver has been used for sensing the rotor position. These position sensors, however, are expensive, require a special arrangement for mounting, and decrease the reliability of the system. For the above-mentioned reasons, there has been an increased interest in developing position sensorless control algorithms [1].

The research, which substitutes observers for speed sensors, has been studied. The adaptive sliding mode observer has been widely considered in the field of the motion control [2~3]. Because the sliding mode observer causes the estimation error to move toward zero by confining it to the sliding surface, the sliding mode observer has a robust estimation performance. In the actual system, however, the sliding mode observer has an inevitable chattering phenomenon, which stresses the system components and excites unexpected instability due to the existence of delay and hysteresis.

To cope with these problems of the sliding mode observer, a binary observer is adopted, and is applied to a speed sensorless vector control of the PMSM [5]. The binary observer consists of a main loop regulator and an auxiliary loop regulator; likewise does the binary controller. Hence it can alleviate the unwanted chattering while retaining the benefits achieved in the sliding mode observer. However, the auxiliary loop regulator continuously changes the gain of the main loop regulator in the domain referred to as the constant boundary layer, and furthermore there are estimation errors. Thus in order to improve the performance of the binary observer, the switching new hyperplane equation of the observer is formed by adding extra integral dynamics to the existing switching hyperplane equation. Because the parameters of the dynamic equations such as machine inertia or viscosity friction coefficient are not well known and these values can be changed during normal operation, there are many restrictions in the actual implementation. Due to these problems, a sensorless algorithm that eliminates the mechanical equation of PMSM is studied by using an adaptive scheme [4]. The proposed adaptive integral binary observer applies an adaptive scheme so that the observer may overcome the problems caused by using the dynamic equations, and the rotor speed is constructed by using the Lyapunov function.

† Corresponding Author: Dept. of Electrical and Electronic Engineering, Inha Univerity, Korea.(cyangk@chollian .net)
* Dept. of Electrical and Electronic Engineering, Inha Univerity, Korea.(youngsk@inha.ac.kr)
** Samsung techwin co., LTD.(yoonseok.han@samsung.co.kr).
Received August 18, 2004 ; Accepted January 20, 2005

In this paper, the design method of the proposed binary observer with the integral augmented switching hyperplane and speed estimator using an adaptive scheme for the sensorless vector control of the PMSM is presented. From experimental results, the estimated performance of the adaptive integral binary observer is compared with that of the adaptive sliding mode observer, and the proposed binary observer has a good estimation performance without chattering problems and estimation errors.

2. Integral Binary Observer

2.1 Integral Binary Observer

In stationary reference frame ($\alpha-\beta$), voltage equation of the PMSM is as follows.

$$\frac{d\mathbf{i}_S}{dt} = \mathbf{A}\mathbf{i}_S + \mathbf{B}\mathbf{v}_S - \mathbf{B}\mathbf{E}_S \tag{1}$$

where, $\mathbf{i}_S = [i_\alpha \quad i_\beta]$: stator $\alpha-$ and $\beta-$ axes currents

$\mathbf{v}_S = [v_\alpha \quad v_\beta]$: stator $\alpha-$and $\beta-$axes voltages

$\mathbf{E}_S = [E_\alpha \quad E_\beta]$: induced voltage

$E_\alpha = -K_E\omega_r \sin\theta_r$

$E_\beta = K_E\omega_r \cos\theta_r$

$\mathbf{A} = (-R_s / L_s)\mathbf{I}$

$\mathbf{B} = (1/L_s)\mathbf{I}$

R_s : stator resistance

L_s : stator inductance

K_E : back EMF constant

ω_r : rotor speed

θ_r : rotor position

$$\mathbf{I} = \begin{bmatrix} 1 & 0 \\ 0 & 1 \end{bmatrix}$$

From (1), the binary observer is composed as the following structure;

$$\frac{d\hat{\mathbf{i}}_S}{dt} = \mathbf{A}\hat{\mathbf{i}}_S + \mathbf{B}\mathbf{v}_S - \mathbf{B}\hat{\mathbf{E}}_S + \mathbf{K}\boldsymbol{\gamma} \tag{2}$$

^ : Estimated value.

$$\mathbf{K} = \begin{bmatrix} k_1 & 0 \\ 0 & k_1 \end{bmatrix}$$

$$\boldsymbol{\gamma} = [\gamma_\alpha \quad \gamma_\beta]$$

Integral switching hyperplanes are defined by

$$\sigma = (\sigma_\alpha, \sigma_\beta) = 0 \tag{3}$$

where, $\sigma_\alpha = -ce_\alpha - \int_0^t e_\alpha d\tau, e_\alpha = \hat{i}_\alpha - i_\alpha$

$\sigma_\beta = -ce_\beta - \int_0^t e_\beta d\tau, e_\beta = \hat{i}_\beta - i_\beta$

c : positive constant

Error dynamics are obtained by subtracting (1) from (2), respectively.

$$\frac{d\mathbf{e}_S}{dt} = \mathbf{A}\mathbf{e}_S - \mathbf{B}(\hat{\mathbf{E}}_S - \mathbf{E}_S) + \mathbf{K}\boldsymbol{\gamma} \tag{4}$$

where, $\mathbf{e}_S = [e_\alpha \quad e_\beta]$

Also, the boundary layer is represented by

$$G_\delta = \sigma^+(t)\sigma^-(t) \le 0 \tag{5}$$

$$\sigma^+(t) = \sigma(t) - c\delta$$

$$\sigma^-(t) = \sigma(t) + c\delta$$

$$0 \le \delta < 1$$

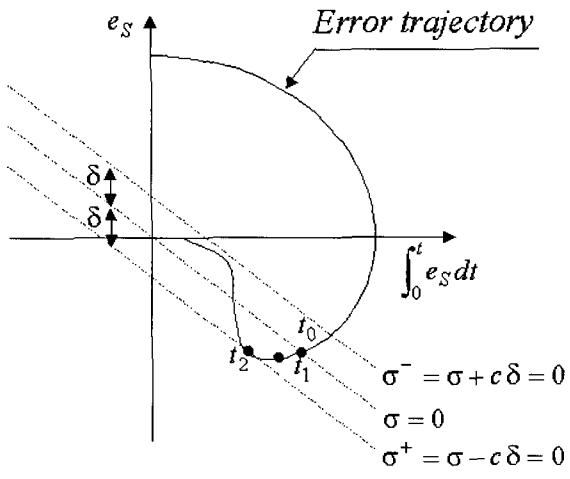

Fig. 1 Phase plane trajectory of the proposed binary observer

The conventional binary observer as compared with the sliding mode observer alleviates the chattering. However, the accuracy of estimation greatly depends upon the thickness of the boundary layer as shown Fig. 1. To improve performance of the estimation, as can be seen in (3), the proposed binary observer is designed with the integral argument switching hyperplane. The configuration of the binary observer is depicted in Fig. 2. Error trajectory departs from an initial position, reaches the boundary layer and converges along the horizontal axis until $\mathbf{e}_S = 0$.

Continuous switching inputs are defined as follows
The main loop regulator:

$$\begin{bmatrix} \gamma_\alpha \\ \gamma_\beta \end{bmatrix} = \begin{bmatrix} \mu_\alpha \mid e_\alpha \mid \\ \mu_\beta \mid e_\beta \mid \end{bmatrix} \tag{6}$$

The auxiliary loop regulator:

$$\begin{bmatrix} \dfrac{d\mu_\alpha}{dt} \\ \dfrac{d\mu_\beta}{dt} \end{bmatrix} = -\alpha \begin{bmatrix} \mu_\alpha + sat(\lambda_\alpha) \\ \mu_\beta + sat(\lambda_\beta) \end{bmatrix} \tag{7}$$

where $\lambda_\alpha = \sigma_\alpha / c\delta$, $\lambda_\beta = \sigma_\beta / c\delta$

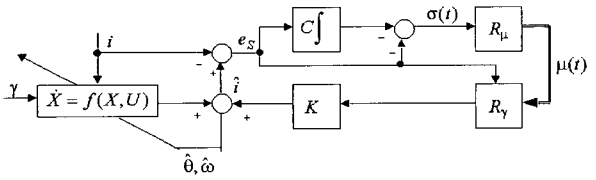

Fig. 2 Block diagram of an adaptive integral binary observer

The block diagram in Fig. 2 represents the proposed binary observer for speed sensorless drives. The condition where all errors exist in the boundary layer G_δ, never leaving the domain G_δ, is referred to as G_δ invariant condition. This condition is similar to the existing condition of the sliding mode. Therefore, the following equation must be satisfied on the boundary of the domain G_δ. Especially, if the auxiliary loop regulator gain α and the main loop regulator gain K are established in order to satisfy (8), the binary observer is as robust as the sliding mode observer.

$$\sigma^+(t)\cdot\dot{\sigma}^+(t) < 0 \quad , \quad \sigma^-(t)\cdot\dot{\sigma}^-(t) < 0 \tag{8}$$

2.2 Derivation of gain K

The main loop regulator gain k_1 can be obtained from the G_δ invariant condition. First of all, if $\sigma_\alpha > 0$, from the inequality (9), the gain k_1 must satisfy (10).

$$\sigma_\alpha \cdot \frac{d\sigma_\alpha}{dt} = \sigma_\alpha \left\{ -c\left[-\frac{R_S}{L_S}\delta + \frac{K_E}{L_S}(\hat{\omega}_r \sin\hat{\theta} - \omega_r \sin\theta) + k_1 v \right] - e_S \right\} < 0 \tag{9}$$

$$k_1 > \frac{1}{(1-h)\delta}\left[\left(-\frac{R_S}{L_S} + \frac{1}{c}\right)\delta + \frac{K_E}{L_S}(\hat{\omega}_r \sin\hat{\theta} - \omega_r \sin\theta) \right] \tag{10}$$

where, $0 < h < 1$

Also, in case of $\sigma(t) < 0$, the result as (11) can be achieved.

$$k_1 > -\frac{1}{(1-h)\delta}\left[\left(-\frac{R_S}{L_S} + \frac{1}{c}\right)\delta + \frac{K_E}{L_S}(\hat{\omega}_r \sin\hat{\theta} - \omega_r \sin\theta) \right] \tag{11}$$

From (10) and (11), k_1 is derived to satisfy (12).

$$k_1 > \frac{1}{(1-h)\delta} \sup_{t \ge t_0} \left| \left(-\frac{R_S}{L_S} + \frac{1}{c}\right)\delta + \frac{K_E}{L_S}(\hat{\omega}_r \sin\hat{\theta} - \omega_r \sin\theta) \right| \tag{12}$$

Symmetrically, (13) is derived

$$k_1 > \frac{1}{(1-h)\delta} \sup_{t \ge t_0} \left| \left(-\frac{R_S}{L_S} + \frac{1}{c}\right)\delta - \frac{K_E}{L_S}(\hat{\omega}_r \cos\hat{\theta} - \omega_r \cos\theta) \right| \tag{13}$$

Therefore, from (12) and (13), k_1 is derived to satisfy (14).

$$k_1 > \frac{1}{(1-h)\delta} \max\left[\sup_{t \ge t_0} \left| \left(-\frac{R_S}{L_S} + \frac{1}{c}\right)\delta + \frac{K_E}{L_S}(\hat{\omega}_r \sin\hat{\theta} - \omega_r \sin\theta) \right|, \sup_{t \ge t_0} \left| \left(-\frac{R_S}{L_S} + \frac{1}{c}\right)\delta - \frac{K_E}{L_S}(\hat{\omega}_r \cos\hat{\theta} - \omega_r \cos\theta) \right| \right] \tag{14}$$

2.3 Derivation of gain α

When $\lambda(t) = \sigma(t)/c\delta$, $\lambda(t)$ is defined as follows

$|\lambda(t)| < 1$ at the domain G_δ

$|\lambda(t)| = 1$ at $\sigma_0^- = 0$ or $\sigma_0^+ = 0$

$\lambda(t') = 1$ at $t = t'$

The gain α can be obtained from (7) and the inequality $-\mu(t')\operatorname{sgn}\lambda(t') < 1-h$.

First of all, if $\sigma(t) > 0$ in integrating (7) for $[t_1, t]$ and then calculating $t = t'$, the following inequality can be achieved:

$$t' - t_1 < \frac{1}{\alpha}\ln\frac{4}{2h-1} \tag{15}$$

where $t > t_1$

t_1 is time when $\lambda(t) = 1/2$

t' is time when $\lambda(t) = 1$

Supposing $-\mu(t')\operatorname{sgn}\lambda(t') = -\mu(t')\operatorname{sgn}\sigma(t') < 1-h$ by using the contradiction method, we can obtain the function $\lambda(t')$ in $[t_1, t']$ for $\lambda(t') \geq 1/2$.

$$\lambda(t') \leq \frac{1}{2} + \frac{1}{c\delta}\overline{K}_0(t_2 - t_1) \tag{16}$$

where,

$$\overline{K}_0 = \max\left[\sup_{t\geq t_0}\left|-c[(-\frac{R_S}{L_S}+\frac{1}{c})\delta + \frac{K_E}{L_S}(\hat{\omega}_r\sin\hat{\theta} - \omega_r\sin\theta) + k_1\gamma_\alpha] - e_\alpha\right|,\right.$$
$$\left.\sup_{t\geq t_0}\left|-c[(-\frac{R_S}{L_S}+\frac{1}{c})\delta - \frac{K_E}{L_S}(\hat{\omega}_r\cos\hat{\theta} - \omega_r\cos\theta) + k_1\gamma_\beta] - e_\beta\right|\right]$$

When we assume the α to be:

$$\alpha \geq \frac{2\overline{K}_0}{c\delta}\ln\frac{4}{2h-1} \tag{17}$$

From (15) through (17), the function $\lambda(t')$ can be given as the following result.

$$|\lambda_0(t')| < 1 \tag{18}$$

Thus, (18) has a contradiction for the equation $\lambda(t') = 1$. This means that if inequality (17) is always held, the magnitude of $\mu(t)$ must have the following relations:

$$|\mu(t)| \geq 1-h \tag{19}$$

2.4 Estimator of speed

In order to estimate the rotor speed, the Lyapunov function is used. The Lyapunov function V is chosen as

$$\mathbf{V} = \frac{1}{2}\mathbf{e}_S^T\mathbf{e}_S + \frac{(\hat{\omega}_r - \omega_r)^2}{2} \tag{20}$$

Under the assumption that the rotor speed is constant within one estimation period, derivation of the Lyapunov function becomes:

$$\frac{d\mathbf{V}}{dt} = \mathbf{e}_S^T\cdot\mathbf{e}_S + (\hat{\omega}_r - \omega_r)\cdot\frac{d\hat{\omega}_r}{dt} \tag{21}$$

Substituting (4) into (21), the following equation is obtained

$$\frac{d\mathbf{V}}{dt} = \mathbf{e}_S^T[\mathbf{A}(\hat{\mathbf{i}}_s - \mathbf{i}_s) - \mathbf{B}(\hat{\mathbf{E}}_s - \mathbf{E}_s) + \mathbf{K}\boldsymbol{\gamma}] + \Delta\omega_r\frac{d\hat{\omega}_r}{dt} \tag{22}$$

where, $\Delta\omega_r = \hat{\omega}_r - \omega_r$

According to Lyapunov's stability theory, $\frac{d\mathbf{V}}{dt}$ must be obeyed to guarantee that the observer is stable. In order to drive the system to be convergent, that is $\frac{d\mathbf{V}}{dt}$, let

$$\mathbf{e}_S^T[\mathbf{A}(\hat{\mathbf{i}}_S - \mathbf{i}_S) + \mathbf{K}\boldsymbol{\gamma}] < 0 \tag{23}$$

$$\mathbf{e}_S^T[-\mathbf{B}(\hat{\mathbf{E}}_S - \mathbf{E}_S)] + \Delta\omega_r\frac{d\hat{\omega}_r}{dt} = 0 \tag{24}$$

From (23), the following inequality can be derived as

$$k_1 > \frac{1}{(1-h)\delta}\left|-\frac{R_S}{L_S}\delta\right| \tag{25}$$

and then, the observer input gain k_1 must be chosen to satisfy inequalities (14) and (25). Therefore, k_1 is derived to satisfy (26).

$$k_1 > \frac{1}{(1-h)\delta}\max\left[\sup_{t\geq t_0}\left|(-\frac{R_S}{L_S}+\frac{1}{c})\delta + \frac{K_E}{L_S}(\hat{\omega}_r\sin\hat{\theta} - \omega_r\sin\theta)\right|,\right.$$
$$\left.\sup_{t\geq t_0}\left|(-\frac{R_S}{L_S}+\frac{1}{c})\delta - \frac{K_E}{L_S}(\hat{\omega}_r\cos\hat{\theta} - \omega_r\cos\theta)\right|, \left|-\frac{R_S}{L_S}\delta\right|\right] \tag{26}$$

From (24), if $\hat{\theta} \cong \theta$, estimation algorithms of the rotor speed may be derived as

$$\frac{d\hat{\omega}_r}{dt} = \frac{K_E}{L_S}\mathbf{e}_S\begin{bmatrix}-\sin\hat{\theta}_r \\ \cos\hat{\theta}_r\end{bmatrix}$$
$$= -\frac{K_E}{L_S}(e_\alpha \sin\hat{\theta}_r - e_\beta \cos\hat{\theta}_r) \quad (27)$$

The estimated rotor position $\hat{\theta}_r$ is obtained by integrating.

3. Experimental Results

Fig. 3 shows the overall system, which consists of a 1.8kW 8 pole PMSM and a Dynamometer. All of the proposed algorithms are implemented using a TMS320C31 and overall calculations are performed by DSP with the sampling time of 160[μ sec]. A three-phase voltage source inverter is constructed by using the IGBT, and the gate-firing logic to implement space-vector-modulation is developed using the motion coprocessor. Also, to align the initial position with α-axis where the rotor position is zero, the voltage pulse is injected into phase a. The actual parameters of PMSM are listed in Table 1.

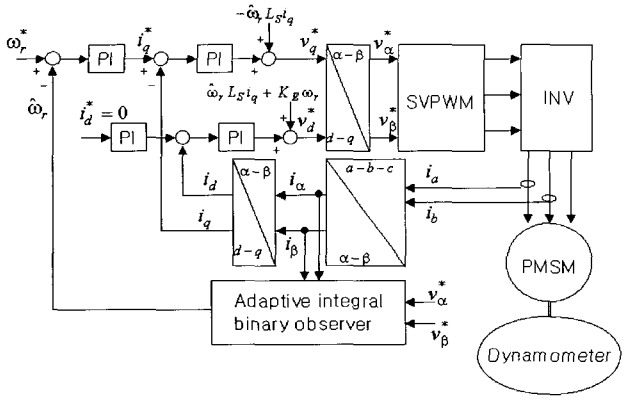

Fig. 3 Block diagram of the proposed algorithm

Table 1 Motor parameters.

Rated power	1.8	kW
Pole number	8	poles
Stator resistance	0.22	Ω
Stator inductance	0.88	mH
Torque rating	5.88	N.m
Rotor inertia	0.00186	[kg·m2]
Back emf constant	0.498	V/rad/s

Fig. 4 indicates the real and estimated speeds and the speed estimation error of the adaptive sliding mode observer, as well as the adaptive integral binary observer with 60% load. The speed estimation error waveform is enlarged ten times larger than the real speed. From Fig. 4, it is known that the estimation performance of the adaptive integral binary observer is superior to that of the adaptive sliding mode observer. This superiority of the adaptive integral binary observer results from the continuous control algorithm of the binary observer and extra integral dynamics that are added to the switching hyperplane equation.

For this experiment, a rapid load change is imposed on the system. In Fig. 5, the estimation performance of the adaptive sliding mode observer and adaptive integral binary observer is illustrated when the load is changed from 0% to 100% at 1000 [rpm], and the robustness of the system to load torque variations is examined. It is known that the robustness of the adaptive integral binary observer is almost identical to that of the adaptive sliding mode observer.

Fig. 6 depicts the real and estimated speeds and the speed estimation error when the speed is reserved from 1500[rpm] to –1500[rpm] with 60% load, and Fig. 7 shows the real and estimated positions under the same condition. The speed estimation error waveform is enlarged to reflect actual size. From Fig. 6 and Fig. 7, although the speed is varied suddenly, the position is estimated by both observers very well.

Fig. 8 and Fig. 9 represent the real and estimated speeds and the real and estimated positions on each observer at the low speed, 50[rpm]. To examine the dynamic behavior of drives, the speed reference is reserved from 50[rpm] to –50[rpm]. Both observers demonstrate lower control performance at low speed regions than at high-speed regions. This is due to poor observability of the rotor angle at low speeds because of the lack of back-emf under the operating conditions. In Fig. 8, the chattering that appeared in the sliding mode observer is almost reduced when the speed is estimated by using the adaptive integral binary observer. The results of the experiments indicate that the adaptive integral binary observer reduces chattering in estimating speed.

Fig. 10 presents the estimation performance of speed when the load is changed from 0% to 34% and returns to 0% at 50[rpm]. In Fig. 10, the successful estimation performance of the rotor speed is shown with a step load at the low speed.

Fig. 11 indicates the absolute values of the percent errors in the rotor speed estimation obtained experimentally, using the adaptive sliding mode observer and adaptive integral binary observer. The absolute values of the estimation percent errors for each rotor speed using the adaptive integral binary observer and adaptive sliding mode observer are nearly identical except in the case of the low speed. These results show that the adaptive integral binary observer has the characteristics of the adaptive sliding mode observer, which is robust for the parameter variation and loads. Also, from Fig. 11, it is known that the

estimation performance of the adaptive integral binary observer is superior to that of the adaptive sliding mode observer during low speed.

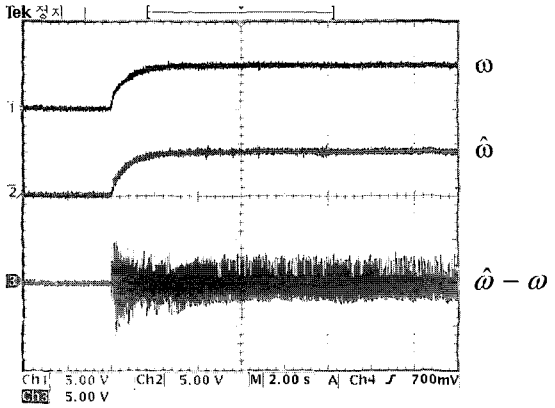

(speed: 500rpm/div, speed estimation error: 50rpm/div)

(a) Adaptive sliding mode observer

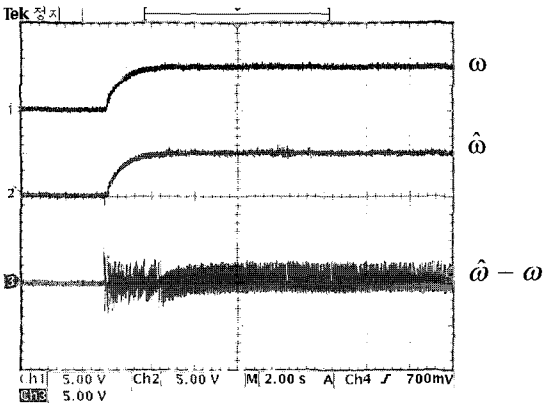

(speed: 500rpm/div, speed estimation error: 50rpm/div)

(b) Adaptive integral binary observer

Fig. 4 Real and estimated speeds and the speed estimation error when the PMSM is derived at 500[rpm] with 60% load

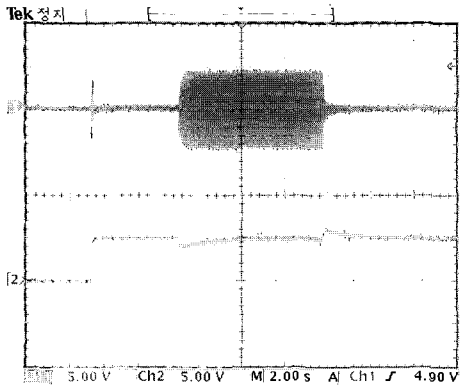

(speed: 1000rpm/div)

(a) Adaptive sliding mode observer

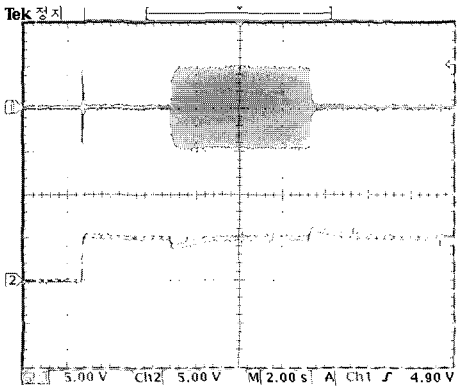

(speed: 1000rpm/div)

(b) Adaptive integral binary observer

Fig. 5 Line current and estimated speed when the load is changed from 0% to 100% and returns to 0% at 1000[rpm]

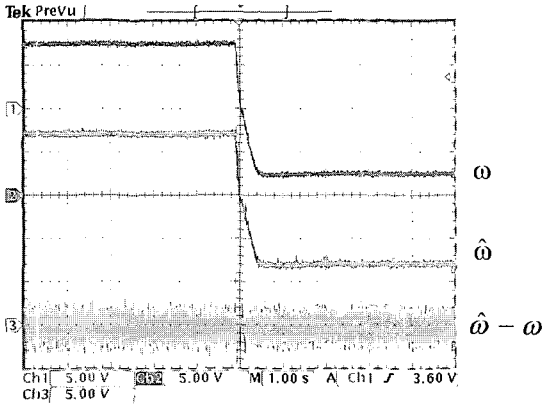

(speed: 1000rpm/div, speed estimation error: 100rpm/div)

(a) Adaptive sliding mode observer

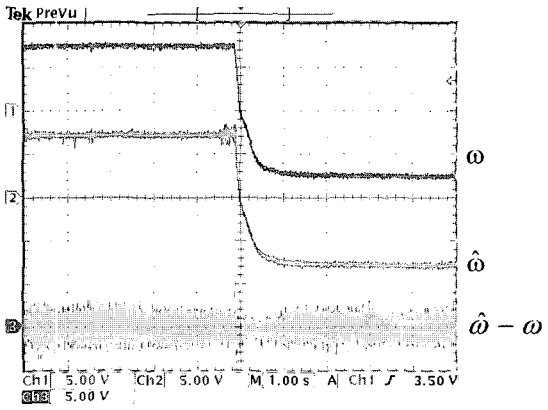

(speed: 1000rpm/div, speed estimation error: 100rpm/div)

(b) Adaptive integral binary observer

Fig. 6 Real and estimated speeds and the speed estimation error when the speed is reversed at 1500[rpm] to -1500[rpm] with 60% load

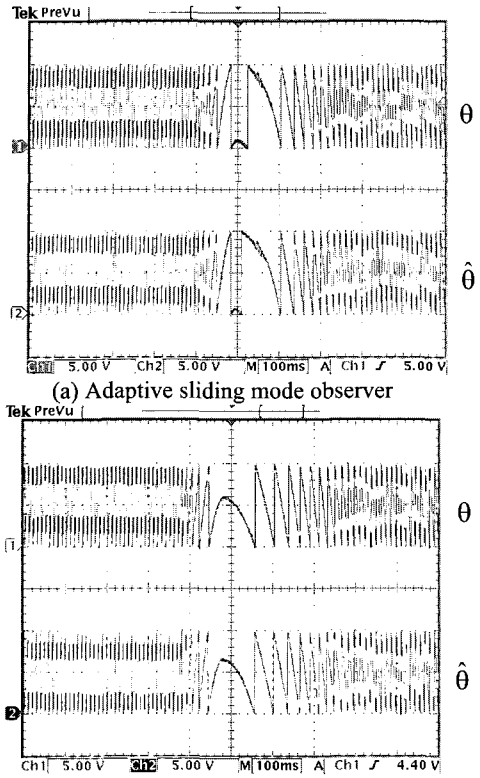

(a) Adaptive sliding mode observer

(b) Adaptive integral binary observer

Fig. 7 Real and estimated position when the speed is reversed from 1500[rpm] to -1500[rpm] with 60% load

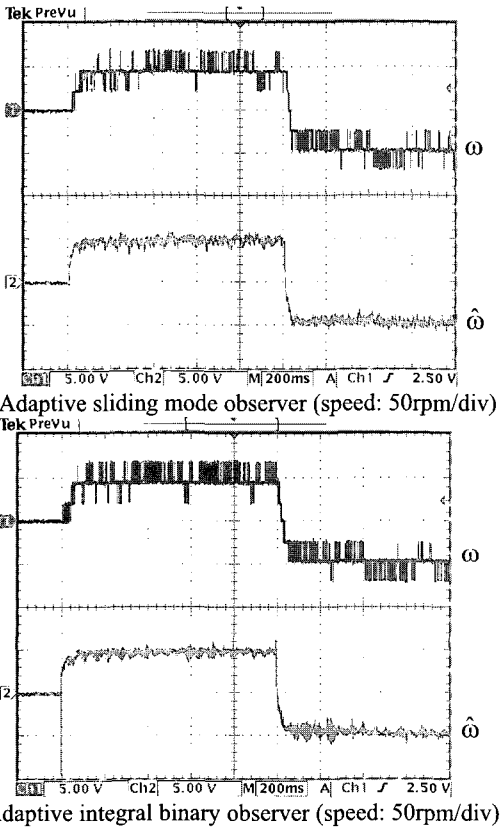

(a) Adaptive sliding mode observer (speed: 50rpm/div)

(b) Adaptive integral binary observer (speed: 50rpm/div)

Fig. 8 Real and estimated speeds when the speed is reversed from 50[rpm] to -50[rpm] with no load

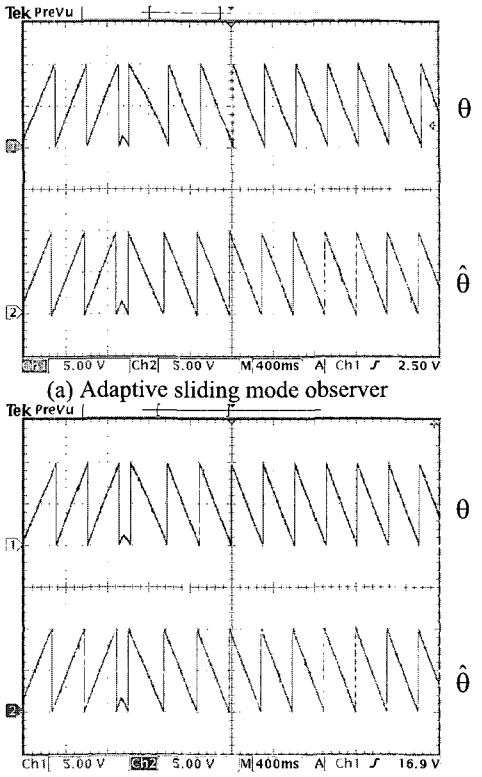

(a) Adaptive sliding mode observer

(b) Adaptive integral binary observer

Fig. 9 Real and estimated positions when the speed is reversed from 50[rpm] to -50[rpm] with no load

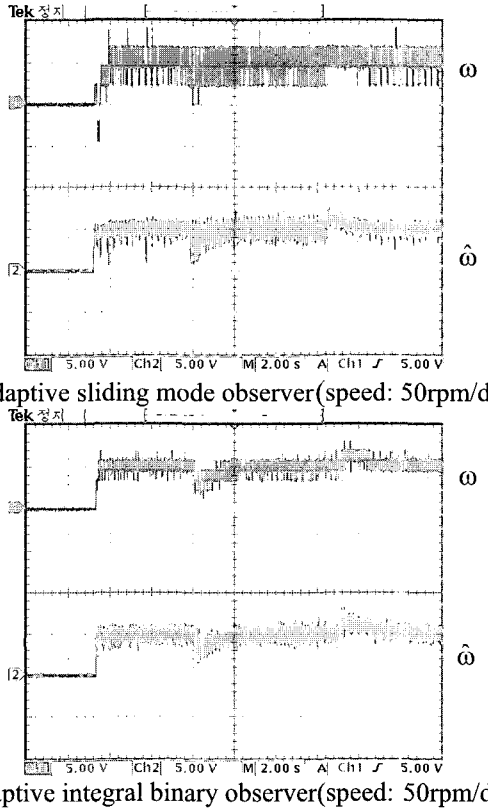

(a) Adaptive sliding mode observer(speed: 50rpm/div)

(b) Adaptive integral binary observer(speed: 50rpm/div)

Fig. 10 Real and estimated speeds when the load is changed from 0% to 34% and returns to 0% at 50[rpm]

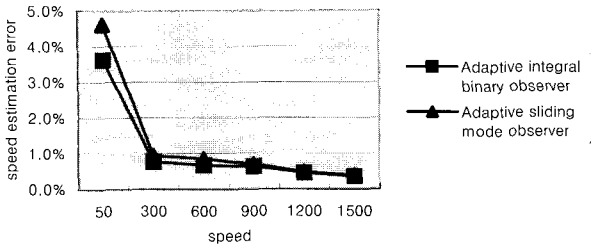

Fig. 11 Absolute value of rotor speed estimation error in a steady state

4. Conclusion

In this paper, a binary observer with integral augmented switching hyperplane is proposed for the accurate and robust speed sensorless control of the PMSM. The observer structure and its design method for the PMSM are developed. The proposed methodology incorporates the Lyapunov algorithm to estimate the rotor speed, so that it can overcome the difficulty that occurs by measuring the motor parameters. The experimental results have confirmed the effectiveness of the proposed strategy. Also, the proposed binary observer that is formed by adding extra integral dynamics to the existing switching hyperplane equation shows the superior steady state performance and the property of chattering alleviation when compared with the adaptive sliding mode observer.

Acknowledgements

This work was supported by a grant from the Korea Research Foundation (KRF-2003-041-D00243).

References

[1] N. Matsui,"Sensorless operation of brushless DC motor drives", in Proc. IECON'93 International Conference on, vol.2, pp739-744, Nov. 1993.

[2] T. Furuhashi, S. Sangwongwanich, S. Okuma, "A position-and-velocity sensorless control for brushless DC motors using an adaptive sliding observer", IEEE Trans. Industrial Electronics, vol.39, Issue.2, pp.89-95, Apr. 1992.

[3] Se-Kyo Chung, Jung-Hoon Lee, Jong-Sun Ko, Myung-Joong Youn, "A robust speed control of brushless direct drive motor using integral variable structure control with sliding mode observer", in Conf. Rec. of the 1994 IEEE, vol.1, pp.393-400, Oct. 1994.

[4] Yoon-Seok Han, Jung-Soo Choi, Young-Seok Kim, "Sensorless PMSM drive with a sliding mode control based adaptive speed and stator resistance estimator", IEEE Trans. Magn., vol.36, Issue5, pp.3588-3591, Sep. 2000.

[5] Young-Seok Kim, Jun-Young Ahn, Wan-Sik You, Kyu-Min Cho,"A speed sensorless vector control for brushless DC motor using binary observer," in Proc. IECON'96, vol.3, pp.1746-1751, Aug. 1996.

[6] S.V. Emelyanov, Binary automatic control systems, Mir Publishers, Moscow, pp14-128, 1987.

[7] Kyeong-Hwa Kim, Myung-Joong Youn, "An Improved Stationary Frame-based Digital Current Control Scheme for a PM Synchronous Motor", JOURNAL OF POWER ELECTRONICS, A PUBLICATION OF THE KORAN INSTITUTE OF POWER ELECTRONICS, vol.1, no.2, pp. 88-98, Oct. 2001.

Yang-Kwang Choi
He received his B.S. and M. S. degrees in Electrical Engineering from Inha University, Korea in 2001 and 2002, respectively.

Young-Seok Kim
He received his B.S. degree in Electrical Engineering from Inha University, Korea in 1977, and his M.S. and Ph.D. degrees in Electrical Engineering from Nagoya University, Japan in 1984 and 1987, respectively. In 1989, he joined Inha University in Korea where he is currently a Professor in the Division of Electrical Engineering.

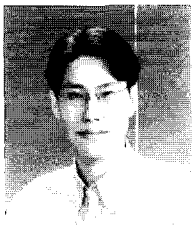

Yoon-Seok Han
He received his B.S., M.S. and Ph.D. degrees in Electrical Engineering from Inha University, Korea in 1995, 1997 and 2001, respectively. He is currently working as a Researcher at Samsung Techwin Co., LTD.